Available online at www.sciencedirect.com
ScienceDirect
Ceramics International 37 (2011) 1153–1160
CERAMICS INTERNATIONAL
www.elsevier.com/locate/ceramint

Synthesis, characterization and photocatalytic properties of sol–gel TiO_2 films

Suzana Šegota [a], Lidija Ćurković [b,*], Davor Ljubas [b], Vesna Svetličić [a], Ivona Fiamengo Houra [c], Nenad Tomašić [d]

[a] *Ruđer Bošković Institute, Bijenička 54, 10000 Zagreb, Croatia*
[b] *Faculty of Mechanical Engineering and Naval Architecture, University of Zagreb, Ivana Lučića 5, 10000 Zagreb, Croatia*
[c] *Brodarski Institute, Av. V. Holjevca 20, 10000 Zagreb, Croatia*
[d] *Institute of Mineralogy and Petrography, Faculty of Science, University of Zagreb, Horvatovac bb, 10000 Zagreb, Croatia*

Received 26 May 2010; received in revised form 23 October 2010; accepted 30 October 2010
Available online 1 December 2010

Abstract

The application of heterogeneous photocatalysis is described as an advanced oxidation process (AOP) for the degradation of the diazo reactive dye using immobilized TiO_2 as a photocatalyst. Starting TiO_2 solutions were prepared with and without the addition of polyethylene glycol (PEG) and TiO_2 films were directly deposited on a borosilicate glass substrate using the sol–gel dip-coating method. The surface morphology and the nanoscale roughness of TiO_2 films were studied by means of atomic force microscopy (AFM). Structural properties of TiO_2 were identified by X-ray diffraction (XRD). The decomposition behaviour of organic compounds from the gels was investigated using thermal gravimetry (TG) and differential scanning calorimetry (DSC). Photocatalytic activities of TiO_2 films in the process of degradation of the commercial diazo textile dye Congo red (CR), used as a model pollutant, were monitored by means of UV/vis spectrophotometry. The kinetics of the degradation of the CR dye was described with the Langmuir–Hinshelwood (L–H) kinetic model.

The addition of PEG to the TiO_2 solution resulted in the changes in the film surface morphology, and affected the ratio of anatase–rutile crystal phases and the photocatalytic activity of TiO_2. The TiO_2 film prepared with PEG is characterized by higher roughness parameters (R_a, R_{max}, R_q, R_z and Z_{max}), a lower amount of the rutile phase of TiO_2, a higher amount of the anatase phase of TiO_2 and a better photocatalytic activity compared to the TiO_2 film without the addition of PEG.

Keywords: A. Sol–gel process; Atomic force microscopy; Photocatalysis; UV/TiO_2; Congo red dye

1. Introduction

Synthetic organic dyes are used in various industries, such as textile industry, leather tanning industry, paper production, hair dye production, etc. Wastewaters containing these dyes may be harmful to the environment and living organisms. Therefore, it is very important to remove or degrade these dyes before discharging them into the environment. In addition to standard technologies for the degradation and/or removal of dyes, several new specific technologies, the so-called advanced oxidation processes (AOPs), have been developed to eliminate dangerous compounds from polluted waters. Heterogeneous photocatalysis, as one of the AOPs, could be effective in the oxidation/degradation of organic dyes. A major advantage of using heterogeneous photocatalysis for this purpose is the total mineralization of organic dyes, which results in CO_2, H_2O and corresponding mineral acids [1–12]. The initial interest in the heterogeneous photocatalysis was aroused in 1972 when Fujishima and Honda discovered the photochemical splitting of water into hydrogen and oxygen by the UV irradiated TiO_2 [13]. After that, research on the heterogeneous photocatalysis started growing rapidly [14] in many areas of water and air treatment technologies.

Titanium dioxide generally exhibits the highest photocatalytic activity of all photocatalysts. The use of TiO_2 as a photocatalyst has been of great interest due to its high activity,

* Corresponding author.
E-mail address: lidija.curkovic@fsb.hr (L. Ćurković).

0272-8842/$36.00
doi:10.1016/j.ceramint.2010.10.034

photochemical inertness, non-toxicity, efficiency, and low cost. Other semiconductors that can be used as photocatalysts are WO_3, SrO_2, ZrO_2, ZnO, Fe_2O_3, CeO_2, CdS, ZnS, etc.

Titanium dioxide occurs in three different crystalline polymorphic forms: rutile (tetragonal), anatase (tetragonal) and brookite (orthorhombic). Among these, the anatase phase usually exhibits the best photocatalytic behaviour, while the rutile phase is the most stable phase. A photocatalyst may be used as a suspension in an aqueous solution or it may be immobilized onto a supporting substrate. The immobilization method is more convenient for practical use since the main problem in the usage of TiO_2 suspended in an aqueous solution is the separation of TiO_2 nanopartices after the photcatalytic reaction and their reuse. Among several deposition techniques, the sol–gel dip-coating method produces films with good photocatalytic properties, large area coatings, with low equipment and production costs [15–18]. The crystal structure and the surface morphology of films influence the photocatalytic efficiency of TiO_2. Atomic force microscopy (AFM) is a very important tool for examining the thin film surface morphology at the nanoscale. During the last decade, a considerable interest has been expressed regarding the application of AFM for structural studies of different materials [19–21].

The aim of this research was to prepare titania films, with and without the addition of PEG, on a borosilicate glass substrate by using the sol–gel dip-coating method and their use as the photocatalysts. Characteristics of these films were analyzed and indentified by means of AFM, X-ray diffraction (XRD), thermal gravimetry (TG) and differential scanning calorimetry (DSC).

Commercial diazo textile dye Congo Red (CR) was used as a model pollutant.

2. Experimental

2.1. Preparation of sol–gel TiO_2 films

TiO_2 films were deposited on two types of borosilicate glass substrates: borosilicate glass tubes (200 mm in height and 30 mm in diameter) and borosilicate glass plates with dimensions of 25 mm × 30 mm × 2 mm. Two borosilicate glass tubes were used as photoreactors and four borosilicate glass plates were used for the characterization of films by means of AFM. The substrates were carefully cleaned prior to the process of deposition. First, the substrates were ultrasonically cleaned in detergent and rinsed with water. Then, they were ultrasonically cleaned in acetone and subsequently in ethanol for 10 min, respectively. Finally, they were thoroughly rinsed with deionised water and dried.

For the preparation of solutions (TiO_2 sols), the following components were used:

- titanium (IV) isopropoxide, TIP ($Ti(C_3H_7O)_4$, $M_r = 284.25$, purity > 98%) as a titanium precursor;
- ethanol, (C_2H_5OH, $M_r = 46.07$) as a solvent;
- acetic acid (CH_3COOH, $M_r = 60.05$) as a catalyst;
- acetylacetone ($CH_3(CO)CH_2(CO)CH_3$, $M_r = 100.12$) for peptization;
- distilled water (H_2O, $M_r = 18.02$) for gelation;
- polyethylene glycol, PEG ($HO(C_2H_4O)_nH$, $M_r = 5000–7000$) as an organic/polymer additive.

In the present study, two sols (solutions) were prepared: sol 1 and sol 2. Sol 1 was prepared by dissolving titanium isopropoxide in ethanol. A magnetic stirrer was used to continuously stir the liquid. Then, acetylacetone, acetic acid, and distilled water were added successively. Sol 1 was stirred vigorously for 2 h and after that it was sonicated for 30 min. Sol 2 was prepared using the same procedure as the one described for sol 1 with only one exception, i.e. the addition of 2 g of polymer–polyethylene glycol (PEG). The molar ratios of components used to prepare both titania coating solutions are shown in Table 1.

Borosilicate glass plates were dipped into sol 1 and sol 2 by a home-made, electrically driven pulley system. Substrates were dipped into the sols at a rate of 10 mm/min, were kept there for 10 min, and then removed at the same rate. Also, sol 1 and sol 2 were each poured into a borosilicate glass tube, kept there for 10 min, and slowly poured out of them. Then, all substrates were dried, first at 100 °C for 60 min, then at 500 °C for 4 h. The dipping process was repeated three times for both solutions.

2.2. Characterization of sol–gel TiO_2 films

The surface topography and the roughness of the TiO_2 films were determined by using a Multimode AFM with a Nanoscope IIIa controller (Veeco Instruments Santa Barbara, CA) with a vertical engagement 125 μm scanner (JV). Contact mode imaging was performed under ambient conditions in air, by using silicon tips (NP, Nom. Freq. 18 kHz, Nom. Spring constant of 0.06 N/m), and at a scan resolution of 512 samples per line. The linear scanning rate was optimized between 1.0 and 2.0 Hz at a scan angle of 0°. Images were processed and analyzed by means of the offline AFM NanoScope software, version 5.12r5. Particle dimensions of the granular microstructure of the TiO_2 thin film were determined by means of the Particle Analysis option within the AFM software.

Roughness analysis software option was used to performed roughness analyses on 2 μm × 2 μm imaged surface area for each sol–gel TiO_2 film. Results are presented as the R_a, R_q, R_z, R_{max} and the Z range values.

Table 1
The composition of coating solutions (sol 1 and sol 2) and molar ratios.

Sol	Components, molar ratio					*m*, g
	$Ti(OC_3H_7)_4$	C_2H_5OH	CH_3COOH	$CH_3(CO)CH_2(CO)CH_3$	H_2O	PEG
Sol 1	1	40	0.9	1.3	12.5	0
Sol 2	1	40	0.9	1.3	12.5	2

After the deposition of the sol–gel TiO_2 coating onto glass substrates, the remaining amount of solutions (sol 1 and sol 2) was dried at 60 °C for 24 h in order to produce dried gels. Some amount of the dried gels was used for the analysis by means of thermal gravimetry (TG) and the differential scanning calorimetry (DSC).

The remaining amount of the dried gels was calcined at a temperature of 500 °C for 4 h and prepared in the form of powder. These synthesized powders were analyzed in terms of phase compositions of titania by means of X-ray diffraction (XRD) using a Philips PW 3040/60 X'Pert PRO powder diffractometer (Philips, Almelo, The Netherlands) with CuKα radiation (λ = 1.54055 Å) at 45 kV and 40 mA. The thermal characterization of the TiO_2 samples was carried out by means of differential scanning calorimetry (TA Instruments DSC, Model 2910) and thermogravimetry (SDT, Model 2960).

2.3. Photocatalytic experiments

All experiments were carried out in 0.11 L borosilicate glass tubes as reactors, with 200 mm in height and 30 mm in diameter: (i) a reactor with a sol–gel TiO_2 film without the addition of PEG, (ii) a reactor with a sol–gel TiO_2 film with the addition of PEG and (iii) a borosilicate glass tube without coating. An UV-radiation lamp was placed in the middle of each reactor. The UV radiation reached the TiO_2 photocatalyst through the CR solution, causing the start of the photocatalytic oxidation process.

The CR dye was supplied by ACROS, as a high purity biological stain, and was used as a model compound without further purification. All solutions used in the experiments were prepared by using double distilled demineralised water.

The radiation source was a mercury UV lamp, model Pen-Ray 90-0019-04, with λ_{max} = 365 nm, manufactured by UVP. The UV lamp was placed in the centre of the reactor. The removal of CR was investigated at a temperature of 25 ± 0.2 °C, with continuous purging with air (O_2), using three different conditions: (i) under UV illumination in the absence of sol–gel TiO_2 coatings (photolysis), (ii) in the dark with sol–gel TiO_2 coatings (adsorption) and (iii) under UV illumination in the presence of sol–gel TiO_2 coatings (photocatalysis). The reaction temperature was controlled by the circulation of cooling water. The initial concentration of CR was 17.5 mg L^{-1}. Before turning the UV lamp on, the solution was placed in the dark and covered with aluminium foil. The samples were taken from the reactor for analysis at certain particular intervals (15, 30, 45, 60, 90 and 120 min) and the remaining dye concentration was analyzed with a UV–vis spectrophotometer (HEWLETT PACKARD, Model HP 8430) at 498 nm by using a 1 cm quartz cell. For each condition, repetition tests were done to ensure reproducibility.

3. Results and discussion

3.1. Results of the AFM analysis of sol–gel TiO_2 films

The surface morphologies and the roughness of a single-layer and a three-layer sol–gel TiO_2 film without PEG (film 1) and with the addition of PEG (film 2) are obviously different. The well-defined crystallinity and size of TiO_2 particles were confirmed by the AFM analysis. Figs. 1 and 2 show 3D-views of height data, and the characteristic vertical profiles (''section analysis'') of single nano-particles of the samples (film 1 and film 2), each with a single-layer and a three-layer sol–gel TiO_2 film. As shown in Figs. 1 and 2, the films reveal a homogeneous granular surface. The single-layer TiO_2 film and the three-layer TiO_2 film prepared from sol 1 without the addition of PEG show granular microstructures which are composed of regular particles with heights within a range of 1–8.1 nm and of 1.0–5.4 nm, respectively (Table 2). On the other hand, the single-layer TiO_2 film and the three-layer TiO_2 film prepared from sol 2 with the addition of PEG show granular microstructures which are composed of irregular particles with heights within a range of 2.1–27.3 nm and of 6.9–54.0 nm, respectively. Results indicate that there is a mesoporous structure between the almost monodispersed TiO_2 particles. In addition to particle height, the AFM Roughness analysis also gives the values of the surface roughness parameters. The values of roughness parameters of both investigated films are presented in Table 3. The R_a values of the single-layer and three-layer sol–gel TiO_2 films without PEG are 1.61 nm and 1.00 nm, respectively. The R_a values were lower than those reported (2–4 nm) in the literature [22–24], indicating a possibility that the films are optically smooth [22]. The lower roughness value represents good homogeneity of the TiO_2 particles on the surface [25]. The surface morphology is also affected by the number of layers of TiO_2 film without the addition of PEG, which can be noted in the results of the roughness parameters presented in Table 3. These results agree with the results obtained by section analysis, as presented in Fig. 1.

The addition of a small amount of PEG to a TiO_2 film drastically changes the surface morphology, as well as the roughness parameters. With the addition of PEG, films become rougher. Roughness parameters (R_a, R_{max}, R_q, R_z and Z_{max}) are higher in comparison to the values found in a sol–gel TiO_2 film without the addition of PEG, which is in agreement with the results reported in [26]. Grain boundaries become less sharp and the matrix shows a smoother appearance. These results could be explained by assuming that the PEG adsorbed on the surface of TiO_2 particles produces stabilization by steric effects and leads to the formation of more compact and higher aggregates. Similar roughness surfaces were reported in [27,28].

3.2. Results of the TG and the DSC analysis of TiO_2 gels

Fig. 3 shows the TG-DTA curves of TiO_2 gels of sample 1 (TiO_2 gel prepared without the addition of PEG) and sample 2 (TiO_2 gel prepared with the addition of PEG). The TG curves for both gels show weight loss in two stages. The first weight loss was observed between 25 °C and 125 °C and the second weight loss was recorded in a temperature range from 125 °C to 550 °C. Results of weight loss for both gels are summarized in Table 4. From these results it is clear that both gels have similar

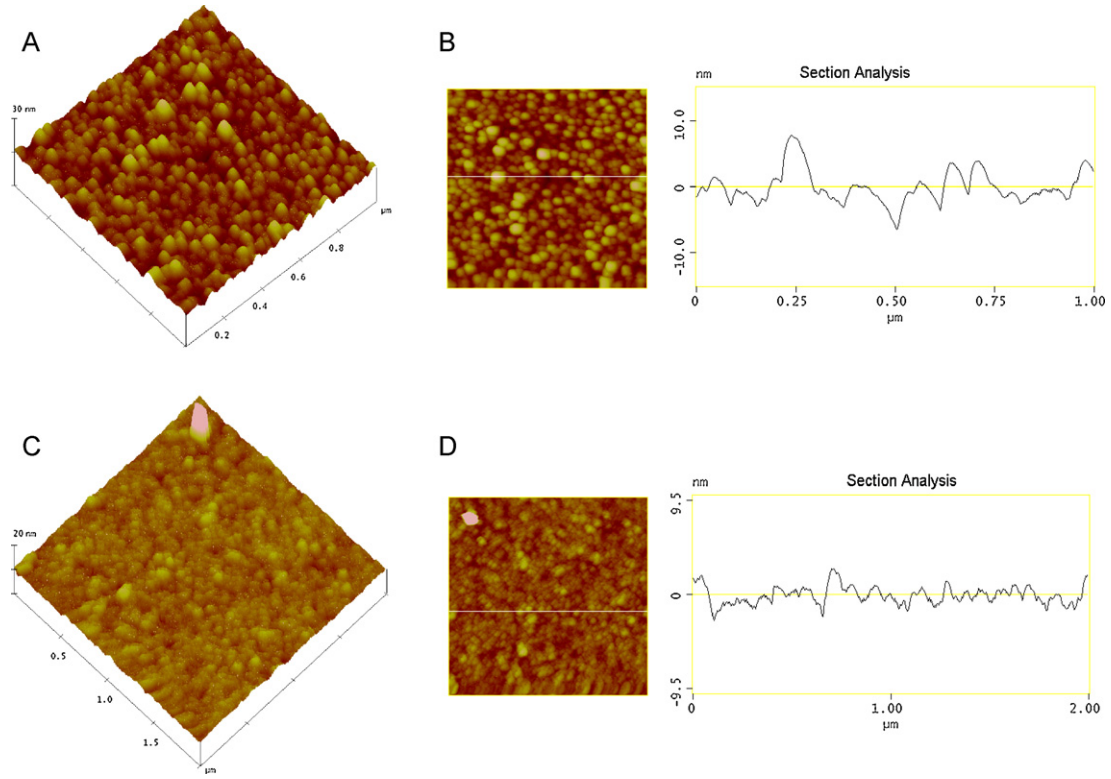

Fig. 1. AFM analysis of film 1 with single-layer and three-layer sol–gel TiO_2 film. Surface topography is presented as a 3D-view of height data and as a height profile along the indicated lines (''section analysis''). (A) Surface topography of a single-layer film (scan size 1 μm × 1 μm, vertical scale 30 nm) and (B) corresponding section analysis. (C) Surface topography of a three-layer film (scan size 2 μm × 2 μm, vertical scale 20 nm) and (D) corresponding section analysis.

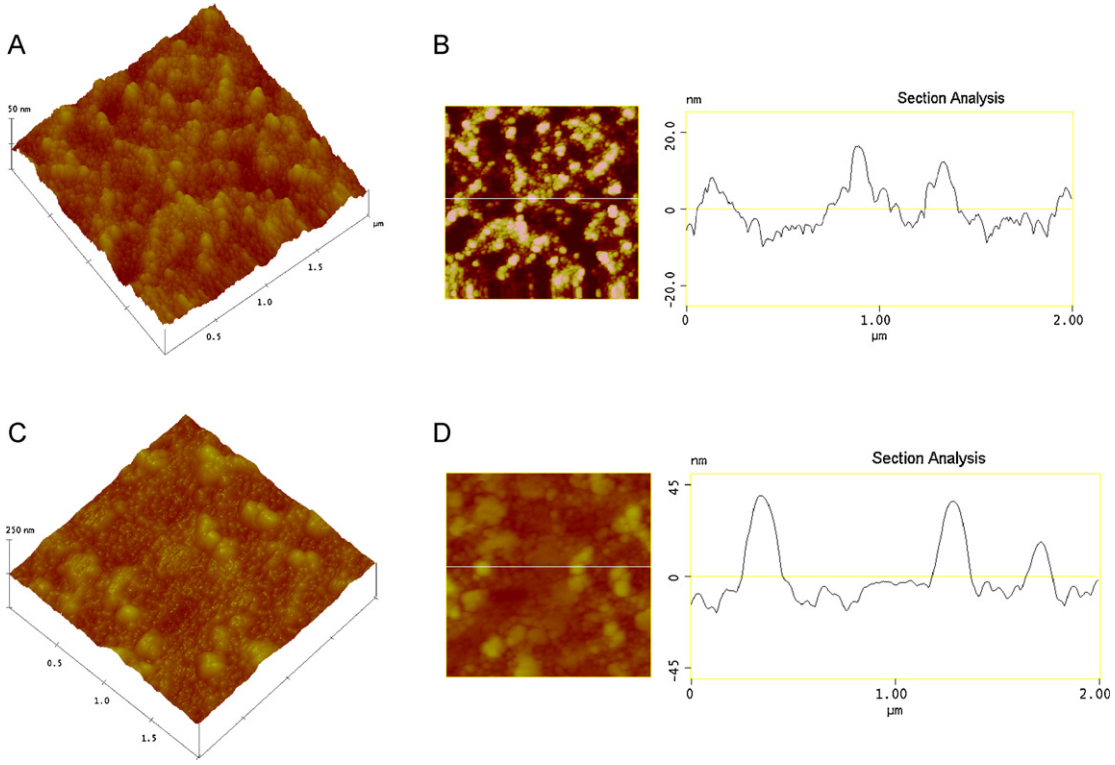

Fig. 2. AFM analysis of film 2 with single-layer and three-layer sol–gel TiO_2 film. Surface topography is presented as a 3D-view of height data and as a height profile along the indicated lines (''section analysis''). (A) Surface topography of a single-layer film (scan size 2 μm × 2 μm, vertical scale 50 nm) and (B) corresponding section analysis. (C) Surface topography of a three-layer film (scan size 2 μm × 2 μm, vertical scale 250 nm) and (D) corresponding section analysis.

Table 2
The number of analyzed TiO_2 particles, their minimum, maximum and mean particle size and corresponding standard deviation obtained from the analyzed area.

Sol–gel TiO_2 film	Particle number	Mean height, (nm)	Minimum (nm)	Maximum (nm)	Stand. deviation
Film 1, 1 layer	473	1.6	1.0	8.1	1.2
Film 1, 3 layers	695	1.3	1.0	5.4	0.4
Film 2, 1 layer	311	6.7	2.1	27.3	5.0
Film 2, 3 layers	258	21.5	6.9	54.0	15.1

Table 3
The roughness parameters of film 1 and film 2 with single-layer and three-layer sol–gel TiO_2.

Sol–gel TiO_2 film	R_a (nm)	R_q (nm)	R_z (nm)	R_{max} (nm)	Z_{max} (nm)
Film 1, 1 layer	1.61	2.08	3.98	20.10	20.90
Film 1, 3 layers	1.00	1.25	1.73	10.50	11.00
Film 2, 1 layer	4.60	5.82	11.00	46.90	46.90
Film 2, 3 layers	9.19	11.90	32.30	73.40	74.30

weight loss (8.13% for the titania without PEG and 9.2% for the PEG-doped titania) in the first temperature interval. The recorded weight loss could be attributed to the evaporation of absorbed water and ethanol in the titania gels and a significant endothermic effect can be found in the corresponding DSC curves (Fig. 4). At temperatures between 125 °C and 550 °C, weight losses of 24.54% and 42.29% were recorded for sample 1 and for sample 2, respectively. That weight loss could be attributed to the combustion of unhydrolyzed isopropoxide ligands and other organic substances bonded to nano-titania particles (for both gels) and the combustion of PEG (for the titania gel doped with PEG). This exothermic process can be found in a corresponding DSC curve.

For sample 1 (TiO_2 gel prepared without the addition of PEG), two overlapping exothermic reactions can be observed. The first, smaller, exothermic peak starts at approximately 200 °C. The second, larger, exothermic peak

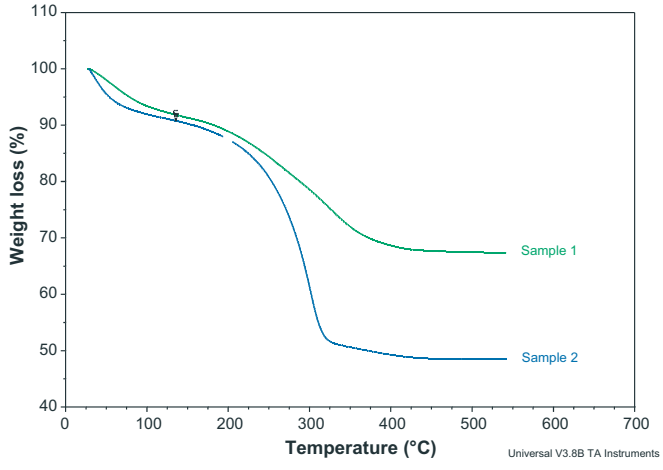

Fig. 3. TG curves of titania gels dried at 25 °C, sample 1 (TiO_2 gel prepared without the addition of PEG) and sample 2 (TiO_2 gel prepared with the addition of PEG).

Table 4
Summarized results of DTA and TGA curves shown in Fig. 3.

Sample	Weight loss (from 25 to 125 °C) (%)	Weight loss (from 125 to 550 °C) (%)	Total weight loss (from 20 to 550 °C) (%)
1	8.13	24.54	32.68
2	9.20	42.29	51.49

was found to start at approximately 330 °C. The exothermic processes are completed at 550 °C. For sample 2 (TiO_2 gel prepared with the addition of PEG), two exothermic reactions can be observed, the same as for sample 1, but at a different temperature range and with a different peak size. The first exothermic peak is larger and occurs at temperatures between 275 °C and 390 °C, while the second exothermic peak is smaller and occurs at temperatures between 400 °C and 550 °C. For both samples of gels, the endothermic peak is attributed to the evaporation of adsorbed water and ethanol. The first exothermic peak is attributed to the combustion and the release of organic substances. The second exothermic peak is ascribed to the transformation of the amorphous phase to the anatase phase and to the small amounts of rutile phase.

3.3. Results of the XRD analysis of TiO_2 nanoparticles

The crystalline structure of calcined TiO_2 samples was studied by XRD. XRD patterns show that titania samples contain two crystalline phases: anatase as a main phase and rutile as a secondary phase (Fig. 5A and B). The sample with the initial sol content of 2 g of PEG has a higher amount of the anatase phase and a lower amount of the rutile phase than the sample without PEG.

3.4. Decolourization kinetics

The results of decolourization of the CR dye by two reactors with the sol–gel coating under UVA irradiation are shown in

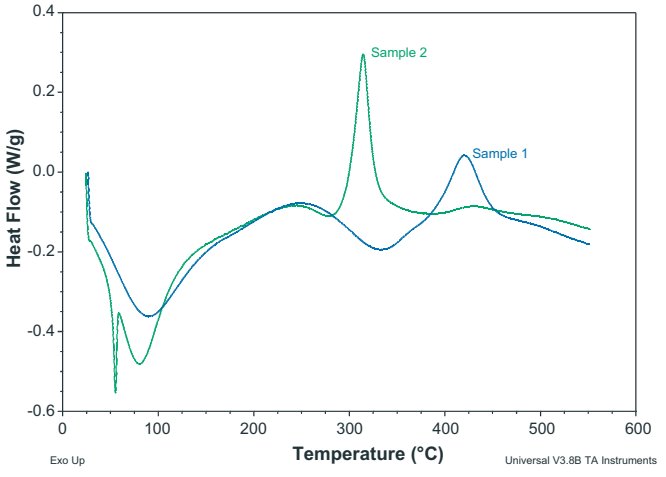

Fig. 4. DCS curves of sample 1 (TiO_2 gel prepared without the addition of PEG) and sample 2 (TiO_2 gel prepared with the addition of PEG).

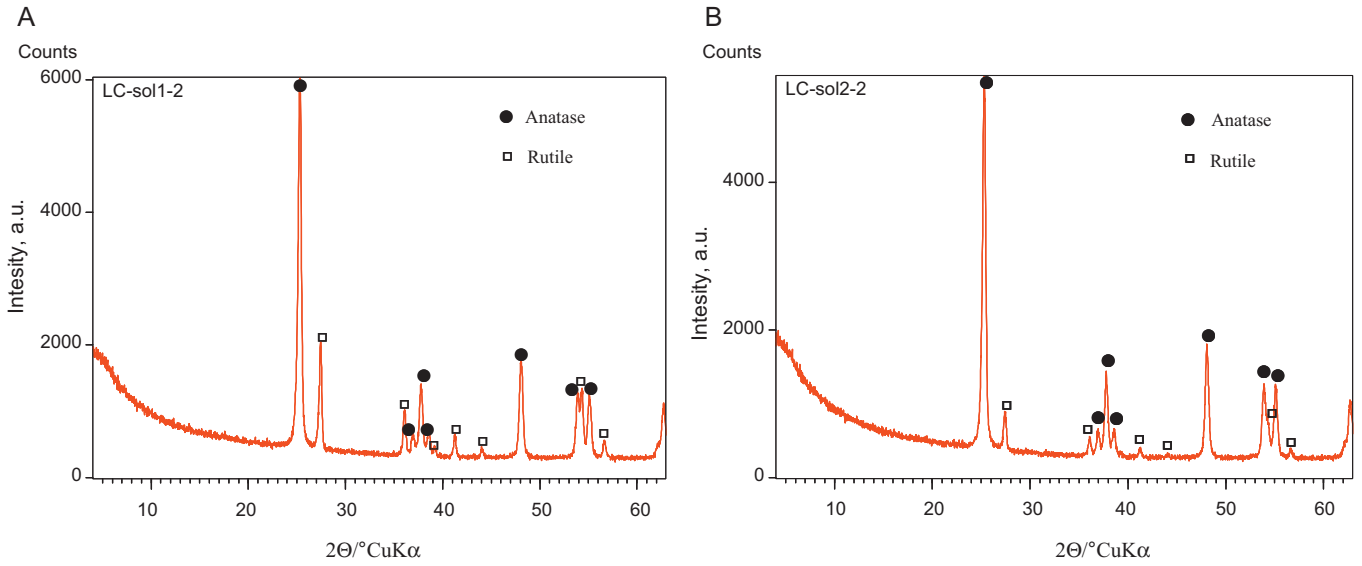

Fig. 5. X-ray diffraction pattern of TiO_2 sample prepared from (A) sol 1 – without the addition of PEG and (B) with the addition of 2 g of PEG to sol 2.

Fig. 6. Also, experiments were performed in both reactors without UVA irradiation as well as in a reactor without the sol–gel TiO_2 coating under UVA irradiation. Under the latter conditions, the decolourization and adsorption effects were negligible. In the presence of the sol–gel TiO_2 coating and the UVA irradiation, the decolourization process progresses proportionally with the irradiation time. Therefore, for these conditions, the pseudo-first order rate constant k' was not determined. Obtained results show that the addition of PEG to the initial sol improves the photocatalytic decolourization of the CR dye. For each experimental condition, three tests were performed simultaneously to confirm the repeatability. Test results confirmed that the used immobilized photocatalyst had retained its constant photocatalytic activity.

The photocatalytic decolourization of the CR dye follows the Langmuir–Hinshelwood kinetics model given by the following equation [22]:

$$-\frac{dc}{dt} = \frac{kKc}{1+Kc} \tag{1}$$

where c is the CR concentration (mg L^{-1}) at a time t (min), k is the reaction rate constant (mg L^{-1} min^{-1}), and K is the adsorption coefficient of CR (L mg^{-1}). After integration, Eq. (1) is transformed into:

$$t = \frac{1}{Kk}\ln\left(\frac{c_0}{c}\right) + \frac{1}{k}(c_0 - c) \tag{2}$$

As the initial concentration (c_0) is a millimolar solution ($c_0 < 0.1$ mmol L^{-1}), the second term on the right-hand side of Eq. (2) is relatively negligible [29,30]. Therefore, Eq. (2) can be further simplified to give an apparent first-order equation:

$$-\ln\left(\frac{c_0}{c}\right) \cong kKt = k\prime t \tag{3}$$

where k' is the pseudo-first order rate constant in min^{-1}.

The pseudo-first order rate constant k' from Eq. (3) is evaluated through the linear regression of $-\ln(c/c_0)$ versus t (and is in compliance with other research data [31,32]). The corresponding values of the pseudo-first order rate constant k' as well as the determination coefficient R^2 are given in Table 5. The results show that the photocatalytic decolourization of the CR dye can be described by the pseudo-first order kinetic model.

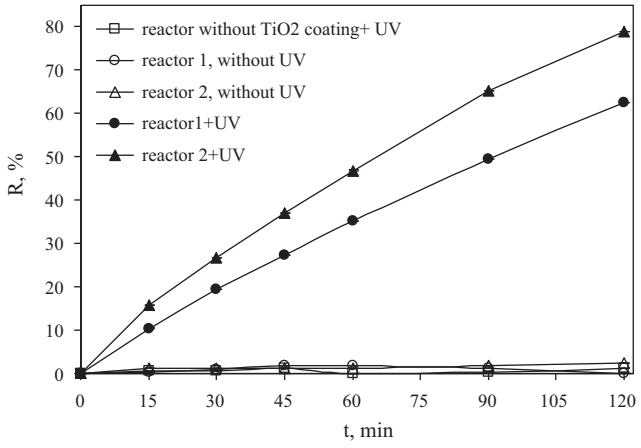

Fig. 6. Photocatalytic decolorization of Congo Red dye (the initial concentration of CR dye is 17.5 mg L^{-1}) under the control conditions (sol–gel TiO_2 coating 1, sol–gel TiO_2 coating 2 only and UV only) and the photocatalytic condition.

Table 5
The pseudo-first order rate constant (k') for the decolorization process of CR aqueous solution in reactor 1 (sol–gel TiO_2 film without the addition of PEG to sol 1) and reactor 2 (sol–gel TiO_2 film with the addition of PEG to sol 2).

Reactor	$k'(\times 10^{-3}, min^{-1})$	R^2
Reactor 1	8.1	0.9942
Reactor 2	12.8	0.9877

The rate constants were calculated to be 8.1×10^{-3} and 12.8×10^{-3} for experiments performed in reactor 1 and reactor 2, respectively (Table 5). The obtained values of the determination coefficient R^2 (Table 5) indicate that the pseudo-first order rate is suitable for describing the photodegradation process of CR photocatalytic degradation with sol–gel TiO_2 coatings as the photocatalyst.

The values of the pseudo-first order rate constants of photocatalytic decolourization are higher for the experiments performed by the sol–gel TiO_2 coating prepared from a sol which contains PEG than for the experiments performed by the sol–gel TiO_2 coating prepared without the addition of PEG.

4. Conclusions

This paper presents the results of the photodegradation process of a diazo Congo Red (CR) dye aqueous solution in the presence of UV irradiation, oxygen and a sol–gel TiO_2 ceramics film. Two sol–gel TiO_2 films were prepared. The first sol–gel TiO_2 film was prepared from the sol without the addition of polyethylene glycol (PEG) and other one was prepared with the addition of PEG.

The results of AFM analysis confirmed the presence of nano-structured sol–gel titania films on the glass substrate. Roughness parameters (R_a, R_{max}, R_q, R_z and Z_{max}) of a sol–gel TiO_2 film with the addition of PEG are higher than the values for the sol–gel TiO_2 film without the addition of PEG.

The sol–gel TiO_2 films with the addition of PEG have a higher ratio of the anatase/rutile crystal phases than the sol–gel TiO_2 films without the addition of PEG.

The sol–gel TiO_2 film prepared from the sol with the addition of PEG was found to be more photocatalyticly efficient than the sol–gel TiO_2 film prepared from the sol without the addition of PEG.

These results indicate that the photocatalytic properties of sol–gel TiO_2 films depend on the surface morphology and roughness as well as on the ratio of two crystalline phases, the anatase (as a main phase) and the rutile (as a secondary phase).

The surface morphology, the anatase/rutile phase ratio and the photocatalytic properties of sol–gel TiO_2 films change with the addition of PEG to the initial sol.

The mechanisms of photocatalytic oxidation of the Congo Red dye by sol–gel TiO_2 coatings were described by a pseudo-first order kinetic model. The value of the pseudo-first order rate constant of CR dye photocatalytic decolourization is higher for the sol–gel TiO_2 film prepared from the sol which contained PEG ($k' = 12.8 \times 10^{-3}\ min^{-1}$) than for the sol–gel TiO_2 coating prepared without the addition of PEG ($k' = 8.1 \times 10^{-3}\ min^{-1}$).

Acknowledgement

This study was supported by the Ministry of Science, Education and Sports of the Republic of Croatia within the framework of the Projects nos 120-1253092-30, 120-1201833-1789 and 098-0982934-2744.

References

[1] C.A. Martiez-Huitle, E. Brillas, Decontamination of wastewaters containing synthetic organic dyes by electrochemical methods: a general review, Applied Catalysis B: Environmental 87 (2009) 105–145.
[2] Z. Yi, J. Liu, W. Wei, J. Wang, S.W. Lee, Photocatalytic performance and microstructure of thermal-sprayed nanostructured TiO_2 coatings, Ceramics International 34 (2008) 351–357.
[3] Z. Bouberka, S. Kacha, M. Kameche, S. Elmaleh, Z. Derriche, Sorption study of an acid dye from aqueous solutions using modified clays, Journal of Hazardous Materials B 119 (2005) 117–124.
[4] S.A. Alem, H. Sarpoolaky, M. Keshmiri, Sol–gel preparation of titania multilayer membrane for photocatalytic applications, Ceramics International 35 (2009) 1837–1843.
[5] J.P. Scott, D.F. Ollis, Integration of chemical and biological oxidation process for water treatment: review and recommendation, Environmental Progress 14 (2) (1995) 88–103.
[6] M.R. Hoffmann, S.T. Martin, W. Choi, D.W. Bahnemann, Environmental Applications of Semiconductor, Photocatalysis 95 (1) (1995) 69–96.
[7] M.N. Rashed, A.A. El-Amin, Photocatalytic degradation of methyl orange in aqueous TiO_2 under different solar irradiation sources, International Journal of Physical Sciences 2 (3) (2007) 73–81.
[8] I.K. Konstantinou, V.A. Sakkas, T.A. Albanis, Photocatalytic degradation of the herbicides propanil and molinate over aqueous TiO_2 suspensions: identification of intermediates and the reaction pathway, Applied Catalysis B: Environmental 34 (3) (2001) 227–239.
[9] K.H. Wang, Y.H. Hsieh, L.J. Chen, The heterogeneous photocatalytic degradation, intermediates and mineralization for the aqueous solution of cresols and nitrophenols, Journal of Hazardous Materials 59 (1998) 251–260.
[10] J.M. Herrmann, Heterogeneous photocatalysis: fundamentals and application to the removal of various types of aqueous pollutants, Catalyst Today 53 (1999), 115-129.
[11] K.M. Parida, N. Sahu, N.R. Biswal, B. Naik, A.C. Pradhan, Preparation, characterization, and photocatalytic activity of sulphate-modified titania for degradation of methyl orange under visible light, Journal of Colloid and Interface Science 318 (2) (2008) 231–237.
[12] W Su, J. Chen, L. Wu, X. Wang, X. Wang, X. Fu, Visible light photocatalysis on praseodymium(III)-nitrate-modified TiO_2 prepared by an ultrasound method, Applied Catalysis B 77 (3–4) (2008) 264–271.
[13] A. Fujishima, K. Honda, Electrochemical photolysis of water at a semiconductor electrode, Nature 238 (1972) 251–260.
[14] A.L. Linsebigler, G. Lu, J. Yates, Photocatalysis on surfaces: principles, mechanisms, and selected results, Chemical Reviews 95 (1995) 735–758.
[15] L Ćurković, D. Ljubas, H. Juretić, Photocatalytic decolourization kinetics of diazo dye Congo Red aqueous solution by UV/TiO_2 nanoparticles, Reaction Kinetics, Mechanisms and Catalysis 99 (1) (2010) 201–208.
[16] C.M. Ling, A.R. Mohamed, S. Bhatia, Performance of photocatalytic reactors using immobilized TiO_2 film for the degradation of phenol and methylene blue dye present in water stream, Chemosphere 57 (2004) 547–554.
[17] C. Guillard, B. Beaugiraud, C. Dutriez, J.M. Herrmann, H. Jaffrezic, N. Jaffrezic-Renault, M. Lacroix, Physicochemical properties and photocatalytic activities of TiO_2-films prepared by sol–gel methods, Applied Catalysis B: Environmental 39 (4) (2002) 331–342.
[18] J. Yu, X. Zhao, Effect of surface treatment on the photocatalytic activity and hydrophilic property of the sol–gel derived TiO_2 thin films, Materials Research Bulletin 36 (1–2) (2001) 97–107.
[19] E.J. Kontturi, P.C. Thüne, A. Alekseev, J.W. Niemantsverdriet, Introducing open films of nanosized cellulose-atomic force microscopy and quantification of morphology, Polymer 46 (10) (2005) 3307–3317.
[20] A.A. Baker, W. Helbert, J. Sugiyama, M.J. Miles, New insight into cellulose structure by atomic force microscopy shows the Iα crystal phase at near-atomic resolution, Biophysical Journal 79 (2000) 1139–1145.
[21] M. Zaharescu, M. Crisan, Atomic force microscopy study of TiO_2 films obtained by the sol–gel method, Journal of Sol–Gel Science and Technology 13 (1998) 769–773.

[22] P. Chrysicopoulou, D. Davazoglou, C. Trapalis, G. Kordas, Optical properties of very thin (<100 nm) sol–gel TiO_2 films, Thin Solid Films 323 (1–2) (1998) 188–193.
[23] M.A. Hamid, I.Ab. Rahman, Preparation of titanium dioxide (TiO_2) thin films by sol gel dip coating method, Malaysian Journal of Chemistry 5 (1) (2003) 086–091.
[24] K. Jungsuwattananon, S. Saesoo, N. Pimpha, N. Negishi, Characterization and bactericidal activity of thin-film TiO_2 photocatalyst, CMU Journal of Natural Science. Special Issue on Nanotechnology 7 (1) (2008) 25–31.
[25] M. Bernardi, E.J.H. Lee, P.N. Lisboa-Filho, E.R. Leite, E. Longo, J.A. Varela, TiO_2 thin film growth using the MOCVD method, Material Research 4 (3) (2001) 223–226.
[26] P. Alphonse, R. Bleta, R. Soules, Effect of PEG on rheology and stability of nanocrystalline titania hydrosols, Journal of Colloid and Interface Science 337 (2009) 81–87.
[27] J.C. Yu, W. Ho, J. Yu, S.K. Hark, K. Iu, Effects of trifluoroacetic acid modification on the surface microstructures and photocatalytic activity of mesoporous TiO_2 thin films, Langmuir 19 (9) (2003) 3889–3896.
[28] J.M. Valtierra, M. Sanchez-Cardenas, C. Frausto-reyes, S. Calixto, Formation of smooth and rough TiO_2 thin films on fiberglass by sol–gel method, Journal of the Mexican Chemical Society 50 (2006) 8–13.
[29] I.K. Konstantinou, T.A. Albanis, TiO_2-assisted photocatalytic degradation of azo dyes in aqueous solution: kinetic and mechanistic investigations: a review, Applied Catalysis B: Environmental 49 (1) (2004) 1–14.
[30] W.J. Jung, B.H. Noh, S.H. Baek, G.D. Lee, S.S. Park, S.S. Hong, Photocatalytic decomposition of orange II over TiO_2-loaded on SBA-15 prepared using a microwave process, Reaction Kinetics and Catalysis Letters 91 (2007) 223–231.
[31] P. Calza, V.A. Sakkas, C. Medana, C. Baiocchi, A. Dimou, E. Pelizzetti, T. Albanis, Photocatalytic degradation study of diclofenac over aqueous TiO_2 suspensions, Applied Catalysis B: Environmental 67 (2006) 197–205.
[32] I. Arslan, I.A. Balcioglu, D.W. Bahnemann, Heterogeneous photocatalytic treatment of simulated dye house effluents using novel TiO_2-photocatalysts, Applied Catalysis B: Environmental 26 (2000) 193–206.